https://doi.org/10.6113/TKPE.2017.22.3.207

보이스 코일 모터 방식을 이용한 3 자유도 구형모터의 분석

주정현[1], 니구치 노보루[1], 히라타 카츠히로†

Analysis of a 3-Degree-of-Freedom Spherical Actuator using VCM Principle

Junghyun Chu[1], Noboru Niguchi[1], and Katsuhiro Hirata†

Abstract

The superior performance of the spherical actuator is establishing a new trend in the industry. Spherical actuators can perform multiple degrees-of-freedom (DOF) motions by using only one actuator. Therefore, a multi-DOF device using the spherical actuator can reduce weight and simplify the structure. This paper proposes a new spherical actuator that uses the operational principle of a rotational voice coil motor. The effectiveness of the actuator is verified through 3-D finite element method.

Key words: Multi-DOF actuator, Spherical actuator, Electric machines, Finite element analysis, Permanent magnets, Voice coil motor

1. Introduction

Usually, multi-degree-of-freedom (multi-DOF) systems consist of a number of single-DOF actuators, making the structure of these systems complicated. Furthermore, they have a slow response and low positioning accuracy due to their inevitable problems such as a large backlash, non-linear friction and kinematic singularities in the operation range, The number of actuators and the weight of the overall system can be reduced by using a multi-DOF actuator. The spherical actuator is particularly suitable for industrial applications such as robot wrists, elbows, shoulders and eyes[1]. Other applications include a satellite attitude control[2] and in vehicle devices such as adaptive head lamps and side-view mirrors. Due to the numerous possibilities, various types of spherical actuator were developed[3-9]. They are commonly designed based on the operational principle of a synchronous motor. These types of spherical actuators have a large non-linearity of the torque constant with respect to the rotational position of the rotor and low tilt with a large overall size of the actuators. Furthermore, these spherical actuators are complicated and are difficult to control due to magnetic interferences when a high precision are required. Table 1 shows the comparison characteristics of previous motor and proposed motor.

TABLE I
COMPARISON CHARACTERISTICS OF PREVIOUS MOTOR AND PROPOSED MOTOR

	Previous	Proposed
Operating principle	Synchronous motor	Voice coil motor + Synchronous motor
Control	Hard	Easy
Precision	Low	High

One of the spherical actuators in previous studies is designed using the principle of voice coil motor (VCM)[10]. However this actuator has 2-DOF motions, and this actuator cannot move around Z-axis because of the rotor is composed of coils. Table 2 shows the comparison structure of previous motor and proposed motor.

Paper number: TKPE-2017-22-3-4
Print ISSN: 1229-2214 Online ISSN: 2288-6281
† Corresponding author: k-hirata@ams.eng.osaka-u.ac.jp, Dept. of Adaptive Machine Systems, Graduate School of Engineering, Osaka University
Tel: +81-6-6879-7533 Fax: +81-6-6879-7533
[1] Dept. of Adaptive Machine Systems, Graduate School of Engineering, Osaka University
Manuscript received Dec. 19, 2016; revised Jan. 12, 2017; accepted Feb. 4, 2017

TABLE II
COMPARISON STRUCTURES OF PREVIOUS MOTOR AND PROPOSED MOTOR

		Previous	Proposed
Structure		1 rotor, 1 stator	2 rotor, 2 stator
Size (diameter)		100 [mm]	80 [mm]
Motion range	Tilt	30 [degree]	40 [degree]
	Rotation	360 [degree]	360 [degree]

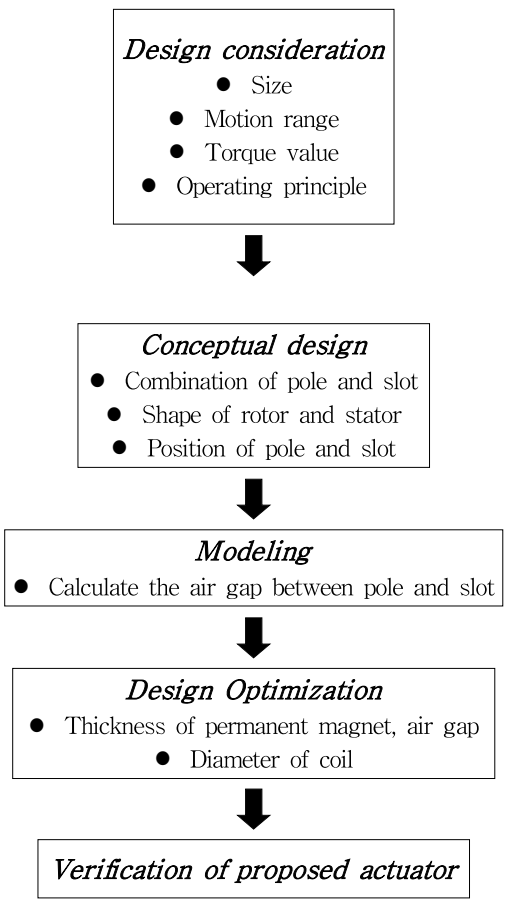

Fig. 1. Design flow chart.

We focus on a large working angle, 3-DOF motion, operating principle of a VCM and high tilt torque with a compact diameter of 80 mm. A VCM can generate forces with a high acceleration, high accuracy and easy control over a limited operation range[11]. The VCM can generate forces that are proportional to the coil currents. Based on these abilities, the proposed spherical actuator has large tilting torques and superior operability. The effectiveness of the actuator is verified through 3-D FEM.

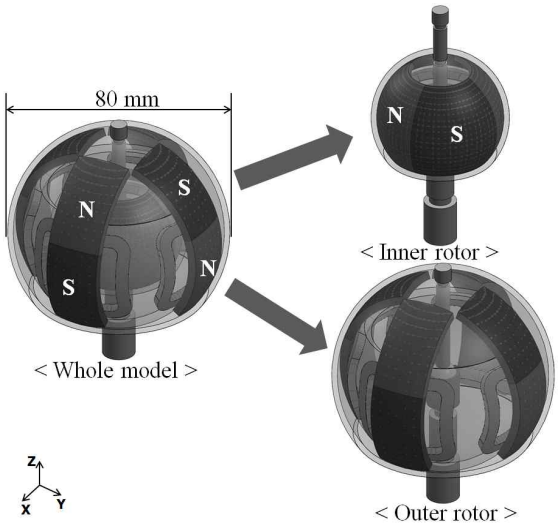

Fig. 2. Schematic diagram of whole model.

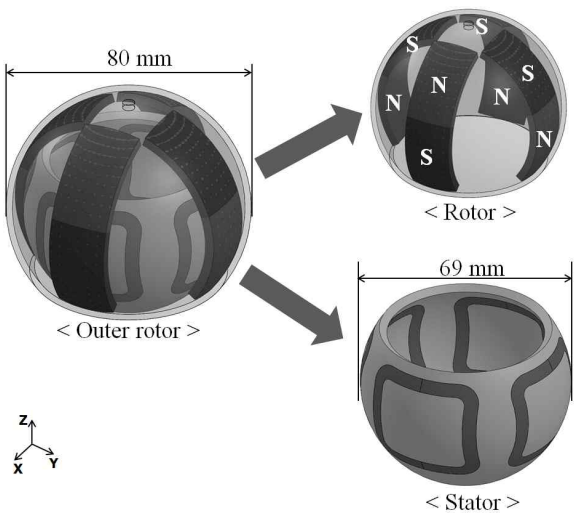

Fig. 3. Schematic diagram of outer rotor.

2. Basic Structure

In order to achieve a large angle of the tilt motion, high tilt torque, easy control, and good dynamic performance, the following design flow chart is considered as shown in Fig. 1.

The proposed spherical actuator consists of two rotors, two stators and motion guide as shown in Fig. 2. The outer rotor and outer stator are used for tilt motions around the X- and Y-axes. The outer rotor consists of 8-pole permanent magnets and 4 coils embedded into the stator as shown in Fig. 3. The inner rotor and inner stator are used for a rotation around the Z-axis, which is an output shaft. The inner rotor consists of 4-pole permanent magnets and 6 coils around the Z-axis as shown in Fig. 4. By using the motion guide, each rotor is fixed in the

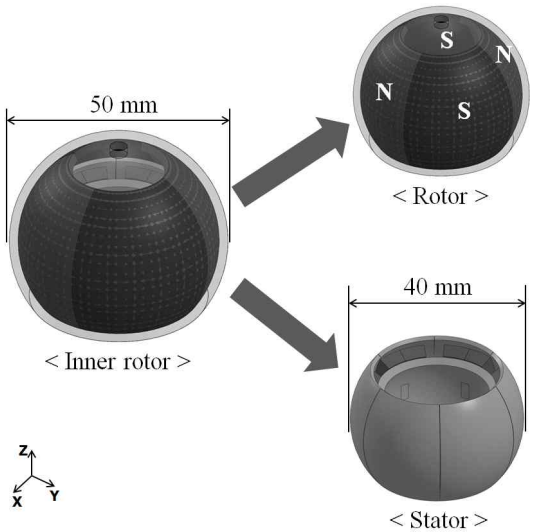

Fig. 4. Schematic diagram of inner rotor.

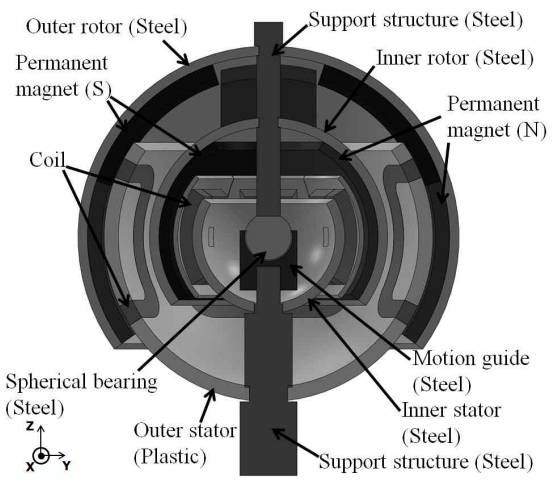

Fig. 5. Y-Z cross section.

same axis and each stator is fixed with each other to maintain the constant air-gap length. The motion guide is consisted of spherical bearing. The ball plunger is also used for maintaining the constant air-gap length. This actuator has enough space between outer rotor permanent magnet (PM) and inner rotor PM in order to decrease the acting force of each PM. The material of the stator of the outer rotor is plastic as shown in Fig. 5. Table 3 shows the detailed specifications of the proposed actuator.

3. Operating principle

The tilting principle around the X- and Y-axes is similar to a rotational VCM. The number of permanent magnets of each side in the outer rotor is the minimum for tilting around X- and Y-axes when using the principle of the VCM.

TABLE III
SPECIFICATIONS OF PROPOSED ACTUATOR

Parameter		Value [mm]
Diameter	Outer rotor	80
	Outer stator	69
	Inner rotor	50
	Inner stator	40
Thickness of permanent magnet	Outer rotor	3
	Inner rotor	2
Width of permanent magnet	Outer rotor	20
	Inner rotor	24.33
Thickness of air gap	Outer rotor ◀▶ Outer stator	0.5
	Outer stator ◀▶ Inner rotor	6.5
	Inner rotor ◀▶ Inner stator	1
	Teeth of inner rotor	0.1

The proposed actuator uses one coil of each side of the outer stator for tilting around X- and Y-axes. The outer coils generate tangential directional forces that cause the tilt torques. Fig. 6 shows the principle of the generation of the tilt torques. Fig. 6 (a) and (b) show tilt motion from 0 to 40 degrees and (c) and (d) show tilt motion from 0 to -40 degrees.

The moving principle around the Z-axis is based on a conventional 4-pole-6-slot permanent magnet synchronous motor as shown in Fig. 7. Torques when the inner rotor rotates around Z-axis are generated by a three-phase current of the inner coils. Both rotors are rotated simultaneously.

4. Characteristic analysis

4.1 Analysis method

An electromagnetic field analysis using 3-D finite el ement method (FEM) is conducted to determine the st atic torque characteristics and the dynamic operating characteristics of the proposed actuator. These charact eristics of the actuator are computed by employing th e Ω-method given in (1) through (3).

$$\mathrm{div}\{\mu(\boldsymbol{T}_m+\boldsymbol{T}_0-\mathrm{grad}\,\Omega)\}=0 \tag{1}$$

$$\left\{\begin{array}{l}\boldsymbol{J}_m=\mathrm{rot}\,\boldsymbol{T}_m\\ \boldsymbol{J}_0=\mathrm{rot}\,\boldsymbol{T}_0\end{array}\right\} \tag{2}$$

$$\boldsymbol{H}-(\boldsymbol{T}_m+\boldsymbol{T}_0)=-\mathrm{grad}\,\Omega \tag{3}$$

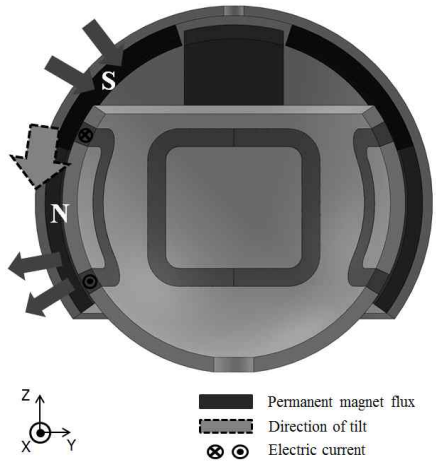

(a) Tilting motion around X-axis on 0 degree

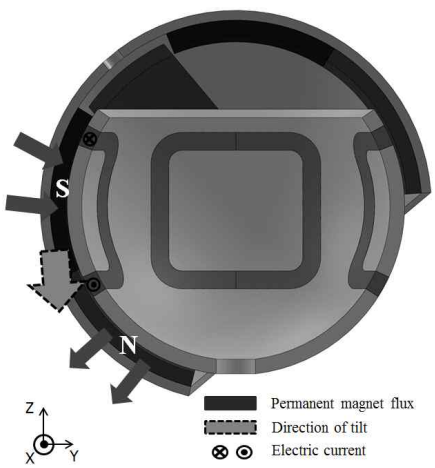

(b) Tilting motion around X-axis on 40 degree

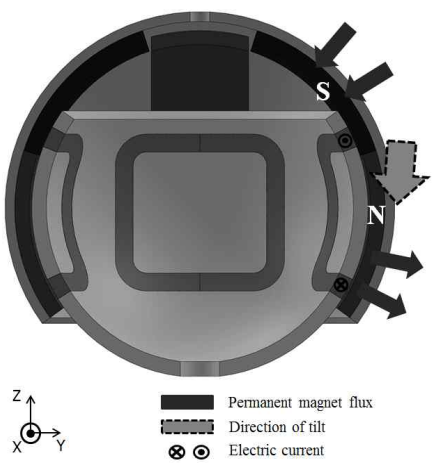

(c) Tilting motion around X-axis on 0 degree

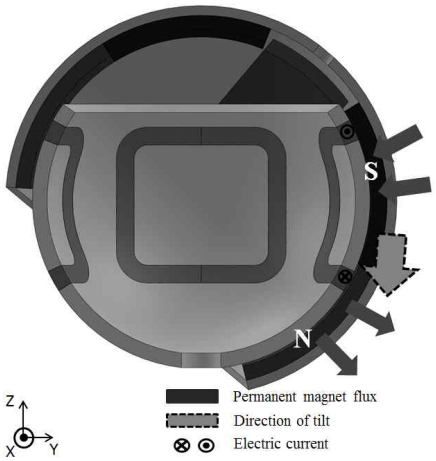

(d) Tilting motion around X-axis on -40 degree

Fig. 6. Principle of generation of the tilt torque.

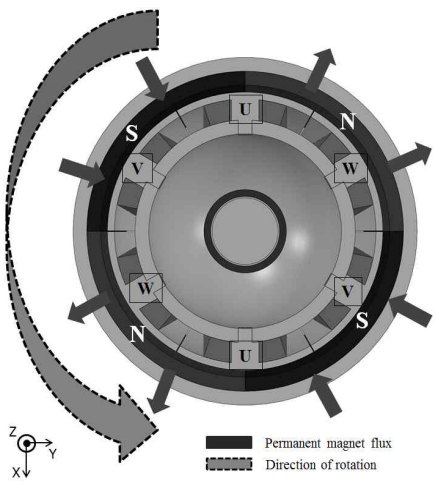

Fig. 7. The rotation motion around Z-axis.

where μ is the permeability, $\boldsymbol{T}_0$ and $\boldsymbol{T}_m$ are the current vector potential derived from the forced current density $\boldsymbol{J}_0$ and equivalent magnetization current density $\boldsymbol{J}_m$, as given in (2), and Ω is the magnetic scalar potential as is given by (3). $\boldsymbol{H}$ is the magnetic field intensity. Equation (1) is computed by using Galerkin's method and then the magnetic force is determined by using Maxwell's stress method. The dynamic characteristics are computed in each axis combined with the motion equation is given as follows.

$$I_i \frac{d^2\theta_i}{dt_i^2} + D_i \frac{d\theta_i}{dt_i} + T_{si} = T_{mi} \quad (i = x, y, z) \tag{4}$$

where I_i is the moment of inertia of the rotor, D_i is the viscous damping coefficient, Θ_i is the rotation angle of the rotor, T_{si} and T_{mi} are the friction torque and the torque acting on the rotor respectively, and i is the rotation axis of the rotor.

The dynamic characteristics are computed in each axis combined with the voltage and mechanical (torque) equation is given as follows.

TABLE IV
ANALYSIS CONDITION OF STATIC TORQUE CHARACTERISTICS

Parameter	Value [Unit]	
Analyzed angle	-40 to 40 [degree]	
Excitation current	2 DC [A]	
Element type	Regular tetrahedron	
Number of element	738,768	
Number of excited coils	4	
Total CPU time	Tilt	14 [hour]
	Rotation	16 [hour]
Number of coil turns	outer coil	600
	inner coil	300

$$V_{to} = r_{in} I_{in} + p\lambda_{in} + E_{ot} + I_{ot} R_{ot} \tag{5}$$

where r_{in} is the armature resistance of inner rotor, I_{in} is the armature current of inner rotor, $p\lambda_{in}$ is the back-emf of inner rotor E_{ot} is the back-emf of outer rotor, I_{ot} is the armature current of outer rotor, and R_{ot} is the armature resistance of outer rotor.

$$T_{to} = \frac{sE_{in}^2 R_{in}}{R_{in}^2 + (sX_{in})^2} \times \frac{3}{2\pi N_{in}} + k_{ot}\phi I_{ot}$$
$$Z_{in} = \sqrt{R_{in}^2 + (sX_{in})^2}, \quad k_{ot} = \frac{P_{ot} \cdot Z_{ot}}{2\pi \cdot A_{ot}} \tag{6}$$

where s is the slip of inner rotor, E_{in} is the back-emf of inner rotor, R_{in} is the armature resistance of inner rotor, Z_{in} is total impedance of inner rotor, N_{in} is the speed in revolution per minute (rpm) of inner rotor, P_{ot} is no. of poles of outer rotor, Z_{ot} is no. of conductors of outer rotor, A_{ot} is no. of parallel paths of outer rotor, I_{ot} is armature current of outer rotor, and ϕ is flux per pole of outer rotor.

4.2 Static Torque Characteristic Analysis

Static torque characteristics analyses were conducted under the following four conditions. In addition to uniaxial motions, the characteristics of luti-axial motions were analyzed to see how a motion around one axis affects a motion around another.

The 3-D finite element mesh model used in these analyses in shown in Fig. 8, and Table 4 shows the analysis conditions to compute the static torque characteristics.

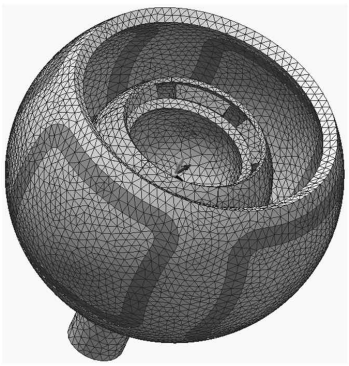

Fig. 8. 3-D mesh model.

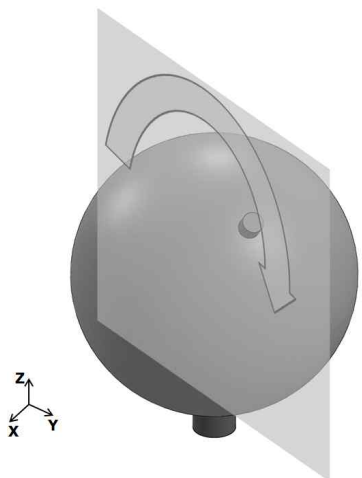

(a) Biaxial tilt motion

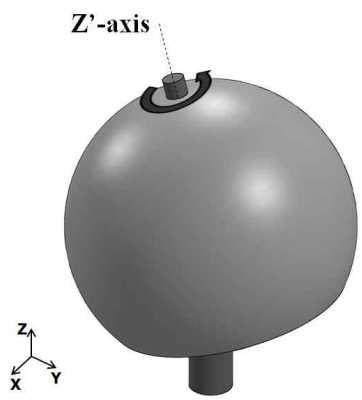

(b) Simultaneous rotation and tilt motion

Fig. 9. Biaxial tilt motion and simultaneous rotation and tilt motion.

The analyzed angular ranges of these analyses are from -40 to 40 degrees for a tilt motion and from 0 to 90 degrees for a rotation motion. Each coil is excited by 2-A DC during tilt motion, and the inner coils are excited by 2-A 3-phase AC during rotation motion. In addition to the output torque characteristics, the cogging torque characteristics are

also computed in each analysis (dashed lines in each figure). The results of the analyses are shown in Figs. 10-15.

4.2.1. Uniaxial tilt motion

From the result of the uniaxial tilt motion shown in Fig. 10, it can be seen that the actuator is easily-controlled during tilt motion. Furthermore the cogging torque of this actuator is relatively small and the equilibrium point is at the center since the cogging torque value is 0, and its gradient is negative at 0 degrees. The average output torque is 0.2 Nm.

4.2.2. Uniaxial rotation motion

Fig. 11 shows the torque characteristics of the uniaxial rotation motion. The fundamental order of the cogging torque is 13, which is the least common multiple of the pole and slot numbers. The fundamental order of the excited torque is also 12 as shown in Fig. 12. This means that the cogging torque is dominant in the excited torque ripple.

4.2.3. Biaxial tilt motion

The analyzed results shown in Fig. 13 are the cogging and output torque characteristics of the biaxial tilt motion. In this analysis, the rotor tilts toward the 45 degrees angle due to the resultant force of the X- and Y-axes motions as shown in Fig. 9 (a). Since all four coils on the stator are excited, the output torque is higher than that of uniaxial motion. Furthermore the cogging torque characteristics during biaxial tilt motion are about the same gradient as that during uniaxial tilt motion. Therefore we can deduce that the cogging torque characteristics will be the same during tilt motion in any arbitrary direction.

4.2.4. Simultaneous rotation and tilt motion

Fig. 14 and 15 are the analyzed results of the simultaneous rotation and tilt motion. Fig. 9 (b) shows that the rotor was rotated around the Z'-axis which is the Z axis that has been rotated 20 degrees around the X-axis. From the analyzed result of the cogging torque, it can be seen that little cogging torque is generated around the Y-axis since the rotor is tilted. This is the force that is trying to rotate the rotor back to its equilibrium position. As for the output torque, the Z'-axis torque is about 0.15 Nm, which is lower than that during uniaxial rotation motion. This is attributed to the decreased area of the coils in the inner stator that is facing the permanent magnets of the inner rotor.

The important information obtained from these results is that the output torque is always positive in all of the analyses. This shows that the actuator can rotate in the analyzed range. In addition to this, a notable characteristic is that the output torque around

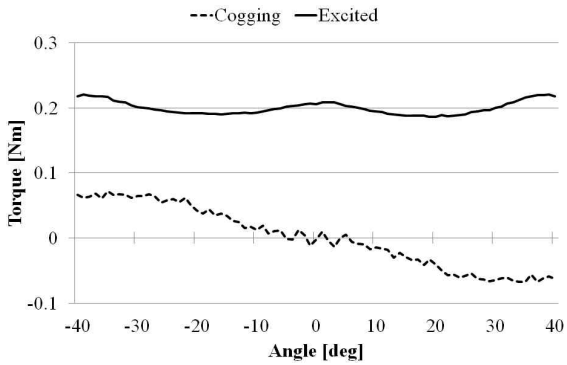

Fig. 10. Torque characteristic of uniaxial tilt motion.

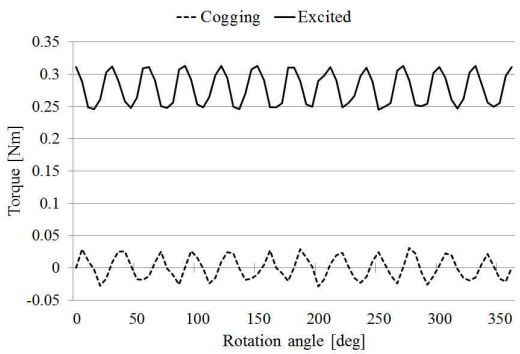

Fig. 11. Torque characteristic of uniaxial rotation motion.

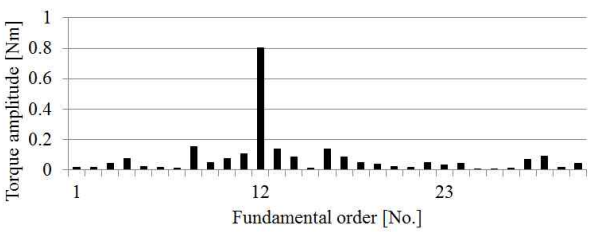

(a) FFT result of cogging torque waveform

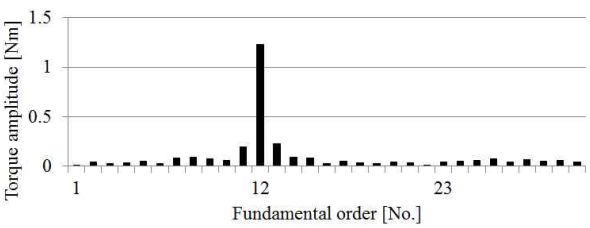

(b) FFT result of excited torque waveform

Fig. 12. FFT results of uniaxial rotation motion.

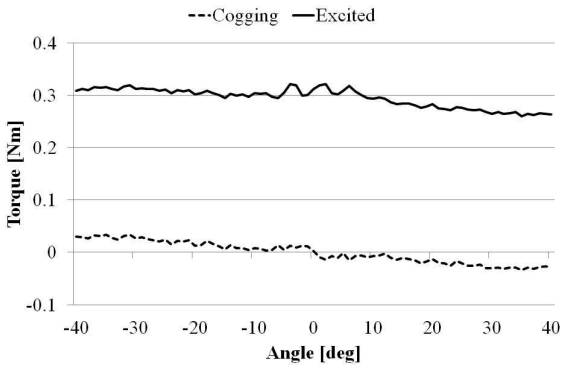

Fig. 13. Torque characteristic of biaxial tilt motion.

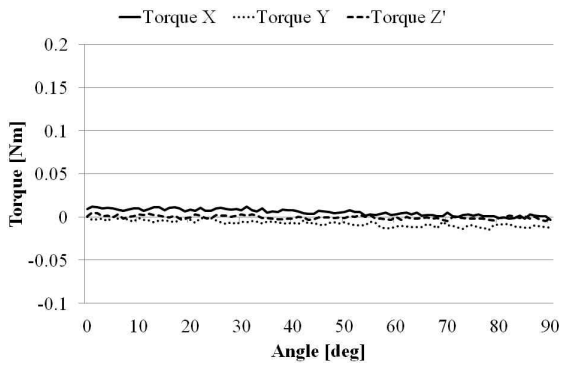

Fig. 14. Cogging torque characteristic of simultaneous rotation and tilt motion.

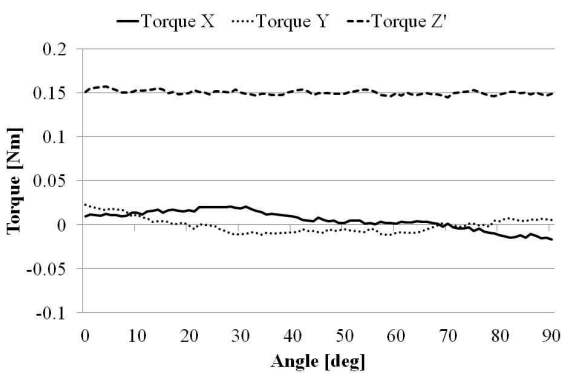

Fig. 15. Excited torque characteristic of simultaneous rotation and tilt motion.

the X-axis during simultaneous rotation and tilt motion (solid line in Fig. 15) is relatively flat and has little ripple. If there is a noticeable ripple, the current for a tilt motion must be adjusted constantly to maintain the tilt angle. Therefore, it can be deduced that simultaneous three degree of freedom control can be easily accomplished and the tilt motion and rotation motion can be controlled independently.

4.3 Dynamic Operating Characteristic Analysis

Dynamic operating characteristics analyses were conducted to confirm how the rotor behaves during each motion. The characteristics were computed under the following three conditions.

The 3-D finite element mesh model is the same as that used during the static torque analyses and Table 5 shows the analysis conditions to compute the dynamic operating characteristics.

The proposed actuator uses the direct control system. A schematic diagram of the direct control system is shown in Fig. 16. In this system, The common function sends the desired degrees, the coordinate formation function defines rotation axis and how many degrees the rotor rotates around axis and calculates position vectors of poles observed in rotor coordinates, the current function produces the current patterns, and the generator produces amplitude for each current patterns.

The outer coils are excited by a 2-A amplitude, DC current for tilt motions, and the inner coils are excited by a 2-A amplitude, 2-Hz frequency three-phase AC for rotation motions. The results of each characteristics analysis are shown in Fig. 17 and 19.

4.3.1. Uniaxial tilt motion

From the result of the uniaxial tilt motion shown in Fig. 17, it can be seen that the rotor moves in a reciprocating motion. Though we can see large initial transient amplitude, the rotor stabilizes subsequently.

4.3.2. Uniaxial rotation motion

In the rotation motion, the rotor should theoretically rotate 180 degrees per second because the frequency of the electrical angle is 2 Hz. As shown in Fig. 18, the analyzed result shows a good agreement with this theoretical value and the rotor(mover) synchronizes with the rotating magnetic field, though small ripples which resulted mainly from the cogging torque can be seen.

4.3.3. Triaxial motion

Fig. 19 shows the analyzed result of triaxial simultaneous motion combining the circular motion and the tilted rotation. This is the motion that we wanted to realize when we first proposed this actuator. From the analyzed result, it can be confirmed that the rotor is rotating around the Z'-axis, and at the same time the Z'-axis is rotating along a circular path. This result shows that simultaneous triaxial motion is possible by just simply combing the current control for each uniaxial motion.

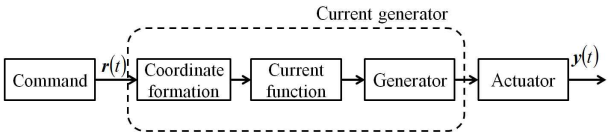

Fig. 16. Block diagram of the direct control system.

TABLE V
ANALYSIS CONDITION OF DYNAMIC CHARACTERISTICS

Parameter	Value [Unit]	
Number of element	738,768	
Number of time steps	Uniaxial Rotation	80
	Other Analyses	160
Total CPU time	Uniaxial Rotation	14 [hour]
	Other Analyses	20 [hour]
Moment of inertia	Tilt	1.62×10^{-4} [kg*m^2]
	Rotation	1.25×10^{-4} [kg*m^2]

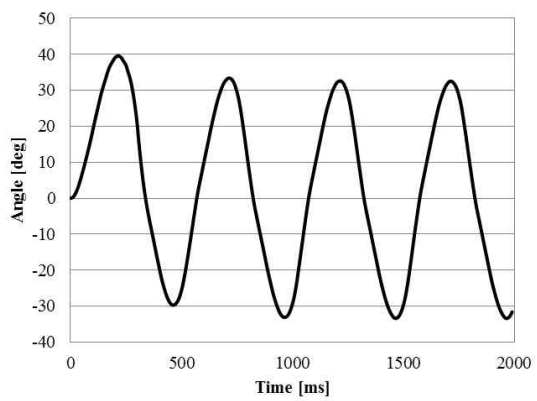

Fig. 17. Operating characteristic of uniaxial tilt motion.

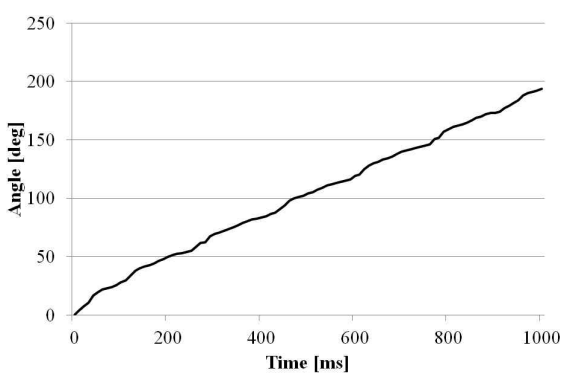

Fig. 18. Operating characteristic of uniaxial rotation motion.

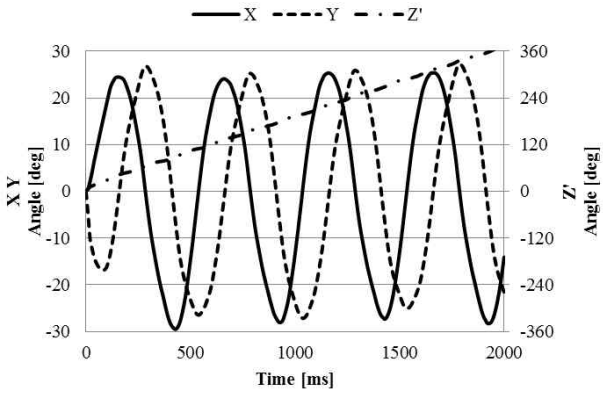

Fig. 19. Operating characteristic of triaxial motion.

5. Conclusion

In this paper, a new multi-degree-of-freedom electromagnetic spherical actuator was proposed to overcome the complex 3-D motion shortcomings of traditional actuators. The basic structure and operating principle of the proposed actuator were presented, and its characteristics were investigated through electromagnetic field analysis using 3-D finite element method. The analysis method was also shown.

The static torque characteristic analyses and the dynamic operating characteristics analyses show that the proposed actuator can rotate around three axes with independent motion. The static torque analyses confirmed that wide angle tilt (-40 to 40 degrees) is possible.

In the future, we are planning to make a prototype and to experiment using a prototype.

References

[1] M. K. Rashid and Z. A. Khalil, "Configuration design and intelligent stepping of a spherical motor in robotic joint," *Journal of Intelligent and Robotic Systems*, Vol. 40, No. 2, pp. 165-181, June 2004.

[2] L. Rossini, O. Ch'etelat, E. Onillon, and Y. Perriard, "Force and torque analytical models of a reaction sphere actuator based on spherical harmonic rotation and decomposition," *IEEE/ASME Transactions*, Vol. 18, No. 3, pp. 1006-1018, May 2012.

[3] E. H. M. Weck, T. Reinartz, G. Henneberger, and R. W. De Doncker, "Design of a spherical motor with three degree of freedom," *Annals CIRP*, Vol. 49, No. 1, pp. 289-294, Jan. 2000.

[4] W. Chen, L. Zhang, L. Yan, and J. Liu, "Design and

control of a three degree-of-freedom permanent magnet spherical actuator," *Sensors and Actuators A: Physical*, pp. 75-86, 2012.

[5] L. Yan, I. M. Chen, C. K. Lim, G. Yang, W. Lin, and K. M. Lee, "Design and analysis of a permanent magnet spherical actuator," *IEEE/ASME Transactions*, Vol. 13, pp. 239-248, 2008.

[6] J. Wang, K. Mitchell, G. W. Jewell, and D. Howe, "Multi-degree-of-freedom spherical permanent magnet motor," *in Proc. Int. Conf. Robot*, pp. 1798-1805, 2001.

[7] L. Yan, I. M. Chen, G. Yang, and K. M. Lee, "Analytical and experimental investigation on the magnetic field and torque of a permanent magnet spherical actuator," *IEEE/ASME Transactions*, Vol. 11, pp. 409-419, 2006.

[8] S. Maeda, K. Hirata, and M. Tong, "Feedback control of electromagnetic actuator with three degrees of freedom using optical image sensors," *Electr. Eng. Japan*, Vol. 181, 2012.

[9] M. Tsukano, Y. Sakaidani, K. Hirata, N. Niguchi, S. Maeda, and A. Zaini, "Analysis of 2-degree of freedom outer rotor spherical actuator employing 3-D finite element method," *IEEE Transactions on magnetics*, Vol. 49, pp. 2233-2236, 2013.

[10] H. C. Kim, H. Y. Kim, D. H. Ahn, and D. G. Gweon, "Design of a new type of spherical voice coil actuator," *Sensors and Actuators A: Physical*, Vol. 203, pp. 181-188, 2013.

[11] J. McBean and C. Breazeal, "Voice coil actuators for human-robot interaction," *IEEE/RSJ Int. Conf (IROS04)*, Vol. 1, pp. 852-858, 2004.

Junghyun Chu

received the M. S. degrees from Hanyang University in 2006. He was a researcher at Dongbu Robot from 2006 to 2008 and KIST (Korea Institute of Science and Technology) from 2009 to 2011. He is currently a Ph. D. student in the Department of Adaptive Machine Systems, Graduate School of Engineering in Osaka University.

Noboru Niguchi

received the B. S., M. S., and D. E. degrees from Osaka University, Japan, in 1998, 2000, and 2011, respectively. He is currently an assistant professor at the Department of Adaptive Machine Systems, Graduate School of Engineering in Osaka University.

Katsuhiro Hirata

received the B. E. degree from Osaka University in 1982 and D. E. degree from Doshisha University in 1996, respectively. He was a researcher at the R&D Lab., Matsushita Electric Work Ltd. from 1982 to 2005. He joined Osaka University in 2005. He is presently a professor at the Department of Adaptive Machine Systems, Graduate School of Engineering in Osaka University.